Simulation of Longitudinal Stability Of Helicopter In Forward Flight

Asst. Lect. Kareem Jawad Kadhim and Asst. Lect. Abid Noor Jameel shahid
Univ. of Baghdad, College of Eng., Mech. Dept.
Kareemjawad@yahoo.com : Abidnoor@yahoo.com

ABSTRACT

The present work describes the development of code for trim and longitudinal stability analysis of a helicopter in forward flight. In general, particular use of these codes can be made for parametric investigation of the effects of the external and internal systems integrated to UH-60 helicopters.

A forward flight longitudinal dynamic stability code is also developed in the work to solve the longitudinal part of the whole coupled matrix of equations of motion of a helicopter in forward flight. The coupling is eliminated by linearization. The trim analysis results are used as inputs to the dynamic stability code. The forward flight stability code is applied to UH-60 helicopter.

Keywords: Helicopter, UH-60, forward flight, hover, longitudinal, trim, dynamic stability

محاكاة الاستقرارية الطولية للهليكوبتر في الطيران الامامي

م.م كريم جواد كاظم وم.م عبد نور جميل شهيد

الخلاصة:

يوضح البحث الحالي تطوير برنامج لتحليل الاستقرارية الطولية للمروحية في الطيران الامامي. بشكل عام، الاستعمال العملي لهذه البرامج يمكن استعمالها في حساب العوامل المؤثرة على الانظمة الخارجية والداخلية للطائرة المروحية من نوع UH-60. تم بناء البرنامج الخاص بالاستقرارية الديناميكية الطولية للطيران الامامي لحل الجزء الطولي للمصفوفة الكاملة لمعادلات الحركة للطائرة المروحية. تم الغاء الارتباط باستخدام الطريقة الخطية. ان نتائج الاستقرارية الساكنة استخدمت كمدخلا الى برنامج الاستقرارية الحركية. تم تطبيق برنامج الاستقرارية للطيران الامامي على الطائرة UH-60.

الكلمات الرئيسية : هليكوبتر ،uh-60 ، الطيران الامامي ، حوامة ، الطولية، ألية الترم ، الاستقرارية الديناميكية

INTRODUCTION

A helicopter is an aircraft that uses rotating wings to provide lift, control, and forward, backward and sideward propulsion. Because of the rotating parts, it has much more capability of maneuvering, while having restrictions on high speeds and high altitudes. Unlike aircraft, the helicopter has the possibilities of vertical landing and takeoff, low speed flight, hover and safe autorotation. For these reasons, helicopters are used in low-altitude; small range combat and search-and-rescue purposes as well as pleasure travels. Although there are some commercial computational fluid dynamics (CFD) programs which may readily be used for helicopter aerodynamic analyses, there are not many off-the-shelf programs for analyzing trim and dynamic stability characteristics of rotorcraft.

Many of these codes interface with each other. One really much needed and extensively used feature that can be benefited from such codes during an aerodynamic analysis phase is the ability to link to some routines through which the trim parameters such as the main rotor tip path plane (TPP) angle, collective angle, longitudinal and lateral cyclic angles, etc. can be acquired and placed very conveniently in hundreds of input files read in by the aerodynamic analysis codes, such as **VSAERO** and **USAERO**. Trim of a helicopter is the situation in which all the forces, inertial and gravitational, as well as the overall moment vectors are in balance in the three

mutually perpendicular axes. Stability is the tendency of a trimmed aircraft to return to the trim condition after a disturbance is applied. Static stability analyzes the initial tendency, while the dynamic stability considers the subsequent motion in time. The aircraft is said to be stable if it returns to equilibrium, and unstable if diverges. The case in which the aircraft has no change in motion is called neutral stability. The motion can be oscillatory or non-oscillatory. Although a full model should be used if a comprehensive helicopter dynamic stability analysis is to be performed, it is possible to look at a partial analysis using engineering judgments. Longitudinal and lateral dynamic stability can be differentiated. Also, since the transition from hover to a low-speed forward flight (e.g. 30 knots) is continuous, the hover and forward flight cases can be analyzed separately. The objective of linked together and used for helicopter trim and dynamic stability analyses. The mathematical development behind all these codes includes many simplifications and assumptions, which are explained in this work.

FORCES AND MOMENTS ACTING ON A HELICOPTER IN FLIGHT

The helicopters come in many sizes and shapes, but most share the same major components. The main rotor is the main airfoil surface that produces lift. The main rotor is the main control mechanism. A helicopter can have a single main rotor, two rotors can be mounted coaxially or they can be in tandem configuration. The main rotor provides the speed and maneuvering controls, as well as the lift needed for the helicopter to fly. The tail rotor is required from the torque effect produced by spinning the main rotor. The rotors are driven through a transmission system by one or two engines, generally being gas turbine engines. The horizontal stabilator serves as a wing which produces lift and helps stabilizing the helicopter in forward direction. The vertical stabilizer generally has a wing-like geometry which produces side force and helps stabilizing the helicopter in lateral directions. The forces and moments acting on a helicopter in trim position are shown. In the figure (1), the vertical stabilizer side force is given as Y_V, in ideal case it is not directed straight to the side and has an angle, but for simplicity purposes it is shown as directed to (-)Y-axis. It is assumed that the tail rotor has no incidence and its thrust vector is given as T_T. The drag forces on all of the components of the helicopter are shown as one vector *D,* which is directed to (–) X-direction for simplicity purposes again. The lift and pitching moment vectors *L* and *M* , stand for the lift and pitching moment produced by the fuselage and the horizontal stabilizer, as well as the wings if exist. Gross weight is shown as *W.* The torque vector produced by the main rotor which is rotating counter-clockwise is shown in order to state the anti-torque effect of the tail rotor.

HELICOPTER ROTOR SYSTEM

There are four primary types of rotor systems: articulated, teetering, semi-rigid and hingeless. The articulated rotor system first appeared on the autogyros of the 1920s and is the oldest and most widely used type of rotor system. The rotor blades in this type of system can move in three ways as it turns around the rotor hub and each blade can move independently of the others. They can move up and down (flapping), back and forth in the horizontal plane, and can change in the pitch angle (the tilt of the blade) as shown in figure (2). In the semi-rigid rotor system, the blades are attached rigidly to the hub but the hub itself can tilt in any direction about the top of the mast. This system generally appears on helicopters with two rotor blades figure (3). The teetering rotor system resembles a seesaw, when one blade is pushed down, the opposite one rises. The hingeless rotor system functions much as the articulated system does, but uses elastomeric bearings and composite flexures to allow for flapping and lead-lag movements of the blades in place of conventional hinges figure (4). Its advantages are improved control response with less lag and substantial improvements in vibration control. It does not have the risk of ground-resonance associated with the articulated type, but it is considerably more expensive. The use of hinges was first suggested by Renard in 1904 as a means of relieving the large bending stresses at the blade root and of eliminating the rolling moment which arises in forward flight, but the first successful practical application was due to Cierva in the early 1920s. The most important of these hinges is the flapping hinge which allows the blade to flap. A blade which is free to flap experiences large Coriolis moments in the plane of rotation and a further hinge – called the drag or lag hinge – is provided to relieve these moments. Lastly, the blade can be feathered about a third axis, parallel to the blade span, to enable the blade pitch angle to be changed. The hinges are shown in Figure (2), where an articulated rotor is demonstrated. The blades of two-bladed rotors

are usually mounted as a single unit on a 'seesaw' or 'teetering' hinge. No lag hinges are fitted. Figure (3) demonstrates a teetering rotor. The semi-rigid rotor resembles the teetering rotor, but now the hub itself also moves about the top of the mast. The hub is strictly attached to the blades.

Hingeless rotors does not have regular flapping and lagging hinges and have blades which are connected to the shaft in cantilever fashion but which have flexible elements near to the root, allowing the flapping and lagging freedoms. A hingeless rotor is shown in Figure (4). The collective changes the pitch angle of the rotor blades causing the helicopter to climb and descend. Through the swash plate, the cyclic controls the pitch angle distribution over the main rotor disc and by this way the disc is tilted sideways or backwards in order to turn, go backwards or change the speed of the helicopter. The anti-torque pedals control the helicopters tail rotor and are used to point the nose of the helicopter in the desired direction. The function of the throttle is to regulate the engine r.p.m.

HELICOPTER ROTOR ERODYNAMICS

There are two basic theoretical approaches to understand the generation of thrust from a rotor system: momentum theory and blade element theory. The momentum theory makes certain additional assumptions, which limit the accuracy:

• The flow both upstream and downstream of the disk is uniform, occurs at constant energy and is contained within a stream tube.

• No rotation is imparted on the fluid by the action of the rotor.

The blade element theory overcomes some of the restrictions inherent in the momentum theory. It considers the local aerodynamic forces on the blade at radial and azimuthally sections, and integrates the forces to find the overall thrust and drag on the rotor. The lift at the blade tips decreases to zero over a finite radial distance, rather than extending all the way out to the edge of the disk. Thus, there will be a reduction in the thrust, or increase in the induced power of the rotor. Forward flight is a more complex situation compared to the hover. Because of the forward velocity, the relative speed of the blade sections differ around the azimuth, and therefore, an imbalance of aerodynamic forces occur along the main rotor disc. The advancing blade has a velocity relative to the air higher than the rotational velocity, while the retreating blade has a lower velocity relative to the air. This lateral asymmetry has a major influence on the rotor and its analysis in forward flight. The dynamic stall phenomenon is another effect coming with the forward flight situation. As blade incidence increases beyond the static stall point, flow reversals are observed in the upper surface boundary layer, but for a time these are not transmitted to the outside potential flow region. Consequently, the lift force goes on increasing with incidence. Eventually, flow separation develops at the leading edge (it may be behind a recompression shock close to the leading edge), creating a transverse vortex which begins to travel downstream. The proximity of the ground to the hovering rotor disk constrains the rotor wake and reduces the induced velocity at the rotor, which means a reduction in the power required for a given thrust; this behavior is called ground effect. The effect exists at low speed forward flight also. Equivalently, ground proximity increases the rotor thrust at a given power.

TRIM AND STABILITY

When all of the forces and moments (i.e. the aerodynamic, inertial and gravitational) about three mutually perpendicular axes are equal, the aircraft is in a state of equilibrium. That equilibrium state is called trim. When propulsive force is greater than drag the aircraft will accelerate; when lift is greater than the weight the aircraft will climb. Each of the blades has two primary degrees of freedom: flapping and lagging, which take place about either mechanical or virtual hinges near the blade root. A third degree of freedom allows cyclic pitch or feathering of the blade. Despite the fact that helicopter blades are relatively flexible, the basic physics of the blade dynamics can be explained by assuming them as rigid. In hovering flight the air loads do not vary with azimuth, and so the blades flap up and lag back with respect to the hub and reach a steady equilibrium position under a simple balance of aerodynamic and centrifugal forces. However, in forward flight the fluctuating air loads cause continuous flapping motion and give rise to aerodynamic, inertial, and Coriolis forces on the blades that result in a dynamic response. The flapping hinge allows the effects of the cyclically varying air loads to reach equilibrium with air loads produced by the blade flapping motion. The flapping motion is highly damped by the aerodynamic forces. The helicopter system can be reduced to 6 DOF like a fixed wing aircraft, three for translation and three for rotation. A statically unstable motion is also dynamically

unstable but a statically stable motion may be either stable or unstable dynamically.

The following general simplifications are implemented in order to make the problem easier:
– The helicopter structure is considered to be absolutely rigid;
– Longitudinal and lateral motions are uncoupled so they can be treated independently;
– No time lags are considered;
– One DOF coming from the throttle is eliminated and the rotor speed is set as constant;
– The blades are assumed as uniform and the lag bending, elastic twist, and axial deflections are disregarded, except the flapping motion;
– The blades do not bend or twist elastically;
– The blades have homogeneous mass distribution;
– Harmonics higher than 2nd order of flapping and cyclic angles are neglected;
– Empirical downwash, side wash, L&D of empennage are used;
– The codes are applicable only to helicopters with single main rotor and a tail rotor;
– Climb angle and sideslip angle are set as zero.

On the basis of these simplifications, the system describing the helicopter motion can be reduced to six equations. These equations are the total forces and moments on each of the coordinate axis:

$$\sum X = 0 \Leftrightarrow X_M + X_T + X_H + X_V + X_F = W.Sin\Theta$$
$$\sum Y = 0 \Leftrightarrow Y_M + Y_T + Y_V + Y_F = -W.Sin\Phi$$
$$\sum Z = 0 \Leftrightarrow Z_M + Z_T + Z_H + Z_V + Z_F = -W.Cos\Phi$$
$$\sum L = 0 \Leftrightarrow L_M + Y_M h_M + Z_M y_M + Y_T h_T + Y_V h_V + Y_F h_F + L_F = 0$$
$$\sum M = 0 \Leftrightarrow \begin{pmatrix} M_M - X_M h_M + Z_M l_M + M_T - X_T h_T + Z_T l_T - X_H h_H \\ + Z_H l_H - X_V h_V + M_F + Z_F l_F - X_F h_F \end{pmatrix} = 0$$
$$\sum N = 0 \Leftrightarrow N_M - Y_M l_M - Y_T l_T - Y_V l_V + N_F - Y_F l_F = 0$$

The forces and moments with the moment arms are demonstrated in Figure (5). The details on the calculations of the forces expressed in the appendix (A).

TRIM CODE

The motion of helicopter in trim is governed by 6 equations, three for total forces acting on the aircraft and three for total moments on each coordinate of the body frame. One can separate the longitudinal and lateral equations and solve the related parameters without much degradation on the accuracy. Therefore, the code solves only for three equations, which are the total forces on the longitudinal and vertical axis and the total moments on the lateral axis.

The code is composed of two models, called CF and XZM. The first model supplies approximate trim parameters which are used as inputs to the second models. The second model, uses those input parameters in order to linearize the non-linear equations of motion and gives the exact parameters. The flow chart of the code is give in Fig (7).

The code is applicable to flight velocities higher than 30 Knots. This is because the angle of attack over the empennage diverges to unstable values. The first model is based on calculating the following two parameters α_{TPP} and T_M, and modifying the other trim variables according to those parameters.

$$\alpha_{TPP} = \tan^{-1}\frac{D_F + H_M + H_T}{W - L_F}$$
$$T_M = \sqrt{(W - L_F)^2 + (D_F + H_M + H_T)^2}$$

here L_F and D_F corresponding to the lift and drag over the fuselage for the empennage on case. The fuselage lift, drag and pitching moment parameters are calculated from experimental data published in previous works of the helicopter. The second model XZM calculates the total forces and moments in x, z and lateral moment directions.

DYNAMIC STABILITY CODE

Longitudinal stability of the helicopter in forward flight is analyzed in two modes: short period mode and phugoid mode. Those frequently oscillatory motions are observed just after a disturbance -like a vertical gust or a longitudinal cyclic step input- occurs. The short period response is based mainly on pitching motion and generally damps quickly. The energy is converted to kinetic energy while descending and the velocity increases; increased velocity increases the thrust and the helicopter is forced to climb; then as the climbing occurs, the velocity is decreased again. The responses of the helicopter after a disturbance are shown in Figure (8).

The dynamic stability code calculates the required stability derivative, the characteristic equation and the roots, and determines about the stability of the helicopter after a step disturbance given by longitudinal cyclic, the collective or due to a vertical gust. The calculation of the stability derivatives are given in appendix A.

TRIMING RESULTS

The helicopter type of UH-60 has input parameters as shown in table (1). The trim results are obtained at velocity 115 Knots and tabled in table (2). The code gives accurate results for the

main rotor parameters as compared with actual results and also for tail rotor thrust and torque.

STABILITY RESULTS OF UH-60 HELICOPTER

It is more logical to find out the static stability characteristics before the dynamic stability is analyzed. Partial derivative of pitching moment of the helicopter with respect to the vertical velocity is a good indicator of the static stability: If the sign of the derivative is positive, then the helicopter is statically stable, and vice versa. In Figure (8), it is clear that the helicopter is statically unstable up to about 130 knots, and becomes stable after that speed. For the dynamic stability, it can be concluded that the helicopter is unstable up 130 knots. Nothing can be said for the speeds higher than 130. The coefficients of the characteristic equation and the Routh's Discriminant values for all forward flight cases are shown in Figure (9). It is seen that until about 110 knots the helicopter shows tendency to go completely divergent in longitudinal aspect. After that speed until about 150 knots, there should be no unstable oscillations, according to the Routh's test. This means that either there are no oscillations, whether divergent or convergent, or the system is stable, whether oscillatory or not. After 150 knots, the helicopter goes divergent again. Looking to the coefficients, the criterion says that if one of the coefficients is negative, than pure divergence or unstable oscillations occur. This is just the case for UH-60 helicopter, since for all forward flight cases there is only one coefficient which is negative, it is C for speeds below 110 knots and D for speeds after 110 knots. Therefore, it can be concluded that for all forward velocity range the helicopter is purely divergent, even though it is statically stable at speeds higher than 130 knots.

The Phugoid motion characteristics change with changing speed (See Figure (10). The period values are very reasonable up to a point where the period goes to very high values. After that speed the attitude changes from divergent to convergent and the period tends to decrease. 110 knots is very likely to be the maximum range speed. The relation which can be occurring between the maximum range speed and the speed which changes the dynamic stability attitude of the helicopter is a good point of discussion. The divergency / convergency characteristics of phugoid motion are pretty obvious in Figure (11). The time-to-double values change sign at the speed the roots change sign. It is obvious that the motion changes attitude from divergent to convergent at about 110 knots. The non-oscillatory roots are also describing some of the dynamic stability characteristics. There is a change in mode from convergent to divergent at the same critical speed, 110 knots, as it is seen at Figure (12). Those roots belong to the short period mode. It can be concluded that, while the phugoid mode shows divergent characteristics up to that critical speed, the short period mode is convergent, and vice versa. This is an interesting result. The change in the X forces per unit change in the forward velocity is called the 'Drag Damping', since the dominant effect comes from the drag forces. The graph below shows that the effect of the drag forces increases as the forward flight increases. The same conclusion can be made for the vertical damping and the pitch damping. Those are the greatest parameters which affect the longitudinal stability of the

CONCLUSIONS

This work describes the development of codes for trim and longitudinal stability analysis of a helicopter in forward flight. The trim analysis results are obtained for a clean UH-60 configuration. One of the trim codes is based on momentum theory. These codes include many simplifying assumptions such as empirical uniform wake model. Nevertheless, application of these codes to some example helicopters indicated reasonably good agreement with the other available data, particularly for the main rotor performance. The results indicated that, improvements are needed in calculation of the torque, and thereby the parameters related to the tail rotor.

Table (1): UH-60 helicopter input parameters.

Description	Algebraic Symbol	Value	Unit
Moment of inertia about y axis	I_{yy}	40000	slug.ft^2
Weight of the helicopter	GW	20000	lb
MAIN ROTOR			
Radius	R_M	30	ft
Chord	c_M	2	ft
Number of Blades	b	4	
Revolution Speed	Ω	21.667	rad/sec
Lift curve slope (NACA 0012)	a	5.73	per radian
Zero Lift Angle of Attack	$\alpha_{L=0}$	0	
Blade twist angle	θ_1	-10	degrees
Height of the rotor above C.G.	h_M	7.5	ft
Long. Distance to C.G.	l_M	-0.4839	ft
Hinge offset ratio	e	0.05	
Blade cut-out ratio	$\frac{x_o}{R}$	0.15	
Flapping inertia of one blade	I_b	2900	slug.ft^2
Polar moment of inertia	J_M	11600	slug.ft^2
Shaft incidence	i_M	0	degrees
TAIL ROTOR			
Radius	R_T	6.5	ft
Chord	c_T	1	ft
Number of Blades	b_T	4	
Revolution Speed	Ω_T	100	rad/sec
Lift curve slope	a_T	6	per radian
Blade twist angle	$\theta_{1,T}$	-5	degrees
Height of the rotor above C.G.	h_T	6	ft
Long. Distance to C.G.	l_T	37	ft
Shaft incidence	i_T	0	degrees
Delta3 angle	δ_3	-30	degrees
Flapping inertia of one blade	$I_{b,T}$	6.25	slug.ft^2
HORIZONTAL STABILIZER			
Span	b_H	9	ft
Area (incl. area inside tail boom)	A_H	18	ft^2
Zero Lift Angle of Attack	$\alpha_{L=0,H}$	0	rad
Moment arm (measured from its rotational axis)	l_H	33	ft
Height above C.G	h_H	-1.5	ft
Incidence	i_H	-3	degrees
VERTICAL STABILIZER			
Span	b_V	7.7	ft
Area (incl. area inside tail boom)	A_V	33	ft^2
Rudder deflection	$\delta_{r,V}$	10	degrees
Moment arm	l_V	35	ft
Height above C.G	h_V	3	ft
FUSELAGE	f_o $\frac{\partial f}{\partial(\alpha_F^2)}$	17.9 0.023	ft^2 ft^2/deg^2
Wetted area	S_{W_F}	680	ft^2
Moment arm	l_F	-0.5	ft
Lift - Empennage on	$\left(L_F/q\right)_{\alpha_F=0}$ $\frac{\partial\left(L_F/q\right)}{\partial\alpha_F}$	-5 111.8987	ft^2 ft^2/rad
Pitch Moment $M_F = q\left\{\left(M_F/q\right)_{\alpha_F=0} + \frac{\partial\left(M_F/q\right)}{\partial\alpha_F}\alpha_F\right\}$	$\left(M_F/q\right)_{\alpha_F=0}$ $\frac{\partial\left(M_F/q\right)}{\partial\alpha_F}$	-160 1789	ft^3 ft^3/rad
Drag divergence Mach #	M_{dd}	0.725	

Table (2): Trim results compared with experimental results of ref (1).

Parameter	theory	experiment	unit
v_1	7.89	7.91	-
a_{1sm}	-0.9	-1.0886	deg
T_m	20544.29	20586	lbf
H_m	-287.58	-145	lbf
Q_m	33512.22	34573	lbf.ft
b_{1sT}	-0.17	-.3094	deg
Q_m	905.45	934.4	lbf.
T_t	629.7	661	lbf
H_t	-19.55	40	lbf
Q_t	120.73	127	lbf.ft
α_f	2.94	3.675	deg
L_f	-480.66	556	lbf
D_f	871.86	867	lbf
M_f	-11248.68	-11722	lbf.ft
Θ	-0.61	-0.9454	deg
α_v	-7.92	8.0743	deg
L_v	-267.46	-273	lbf
D_v	14.30	15	lbf
L_h	287.93	287	lbf
D_h	51.48	58	lbf

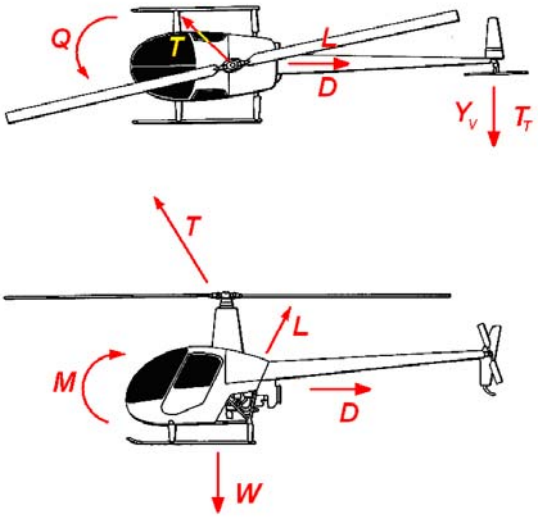

Figure (1): Forces and moments acting on a helicopter.

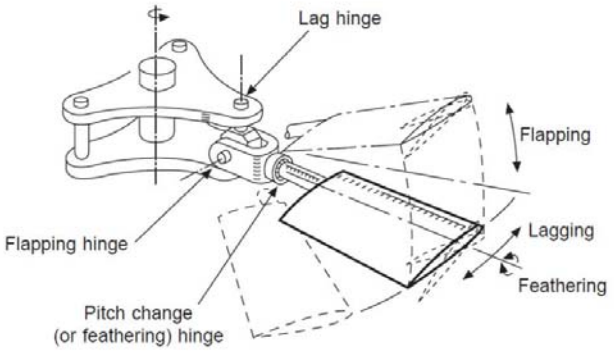

Figure (2): Hinges on an articulated rotor.

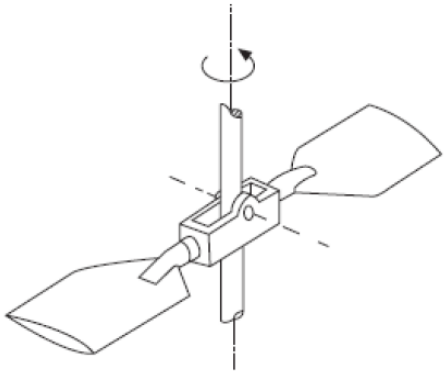

Figure (3): Teetering rotor.

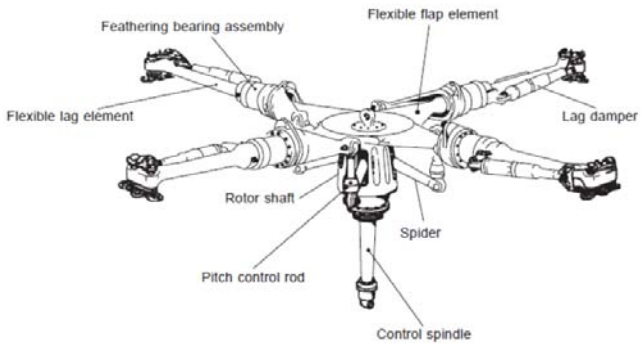

Figure (4): Hingeless rotor.

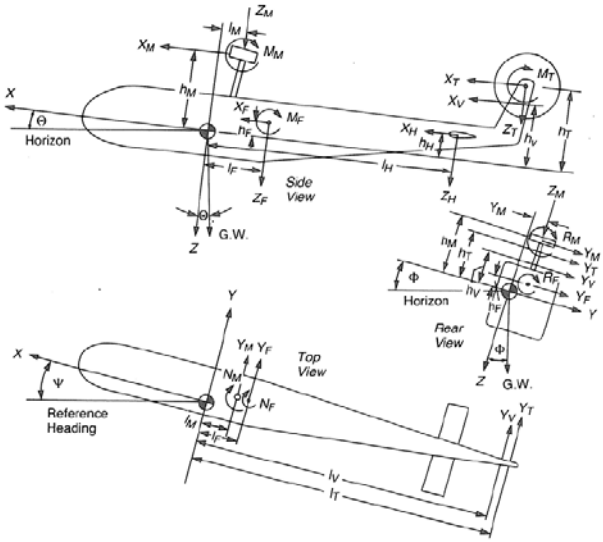

Figure (5): Forces and moments acting on a helicopter [3].

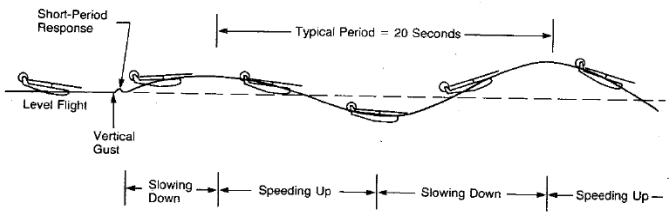

Figure (6): The Phugoid and Short Period Modes.

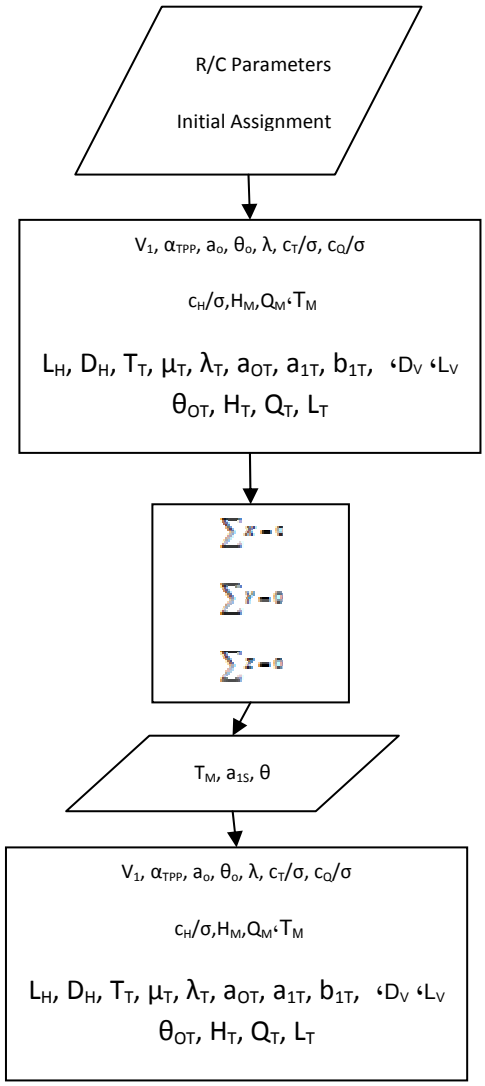

Figure(7): Trim program Flowchart.

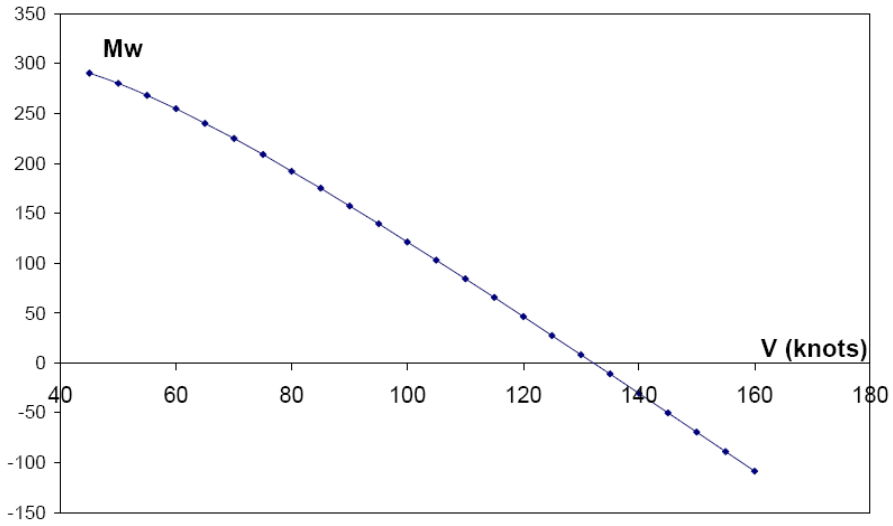

Figure (8): Derivative of pitching moment with respect to the vertical velocity.

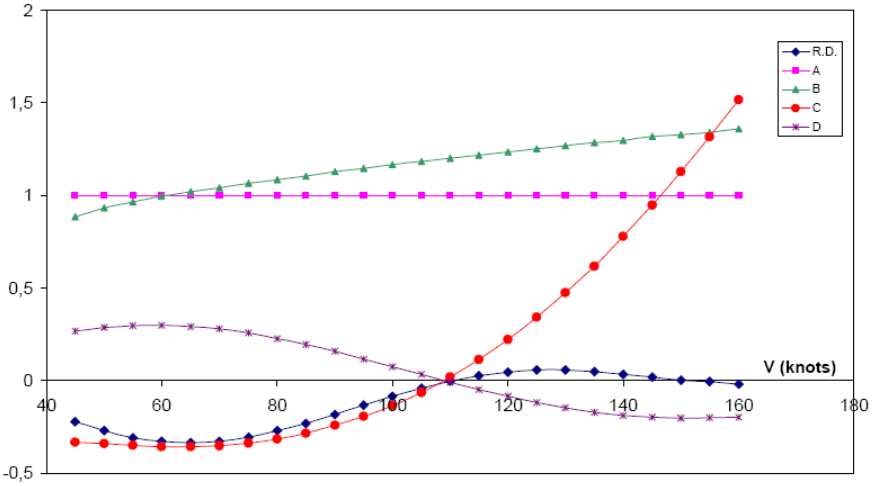

Figure (9): Routh's discriminant and the coefficients of characteristic equation.

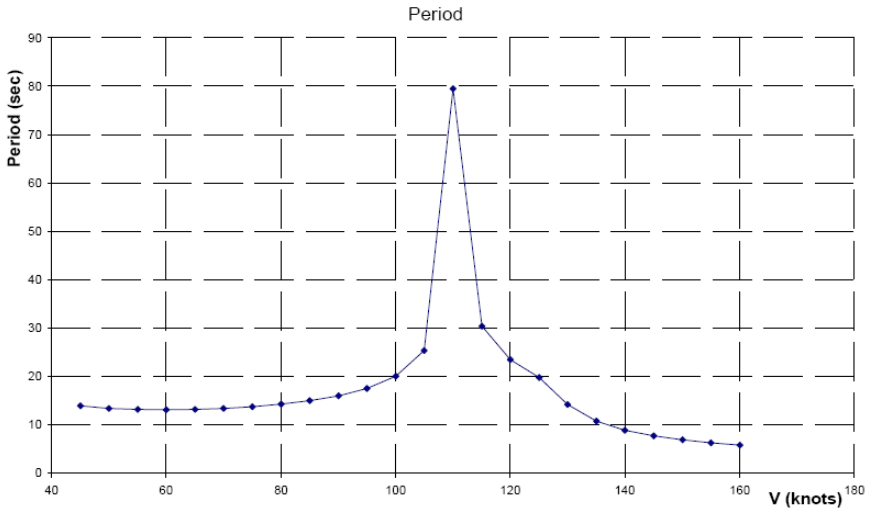

Figure (10): Period values belonging to the phugoid mode.

Figure (11): Time-to-Double values belonging to the phugoid mode.

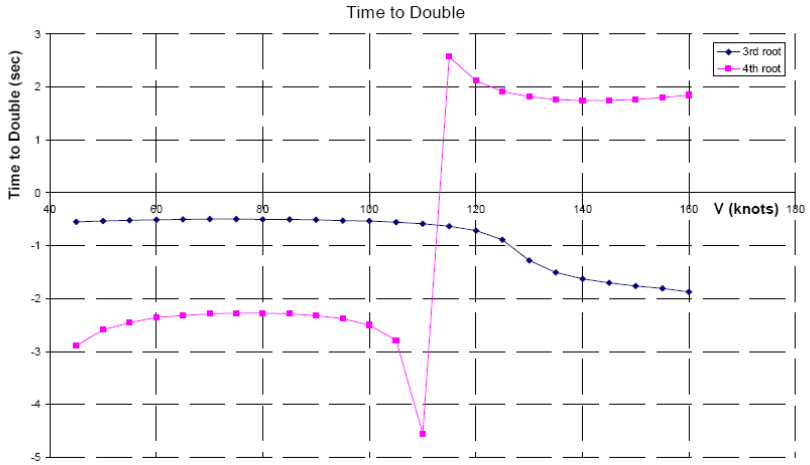

Figure (12): Time-to-double values belonging to the non-oscillatory roots.

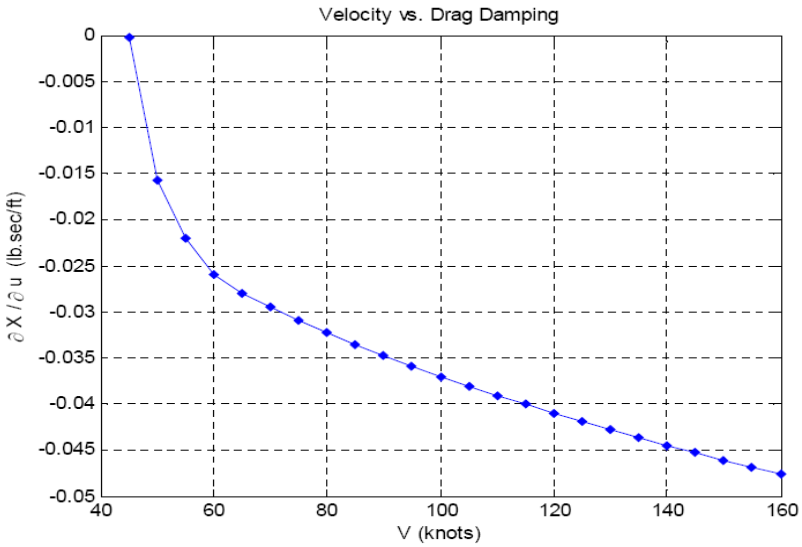

Figure (13): Drag Damping.

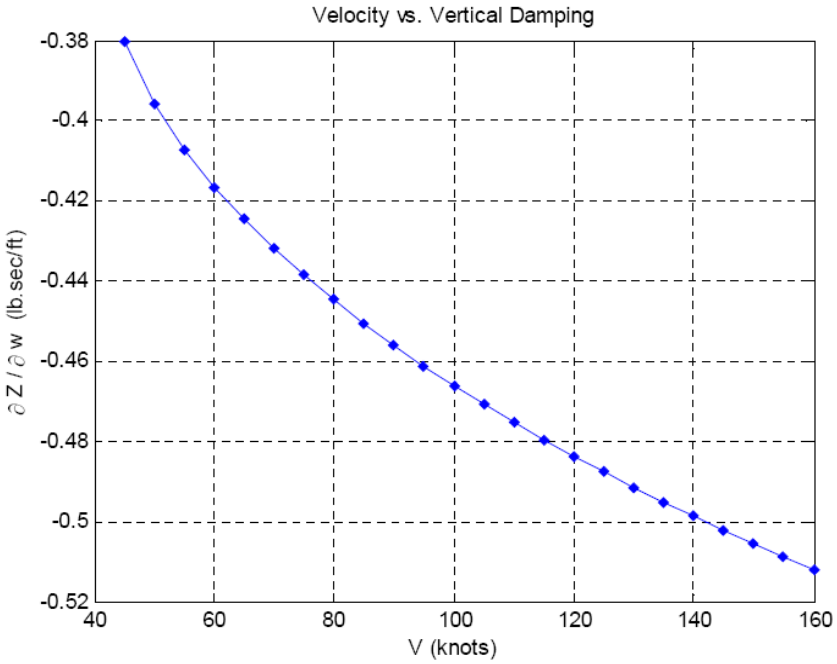

Figure (14): Vertical Damping.

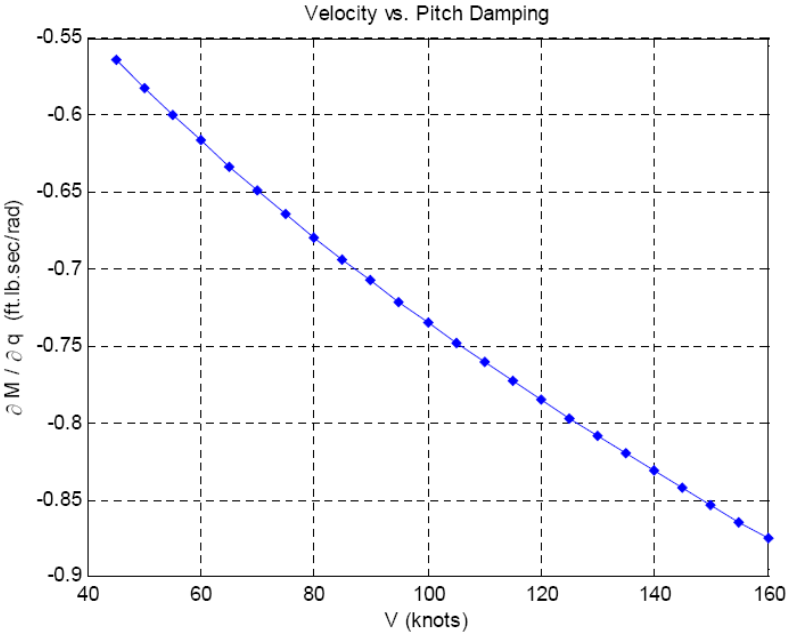

Figure (15): Pitch Damping.

REFERENCES

1.Seddon, J., Basic Helicopter Aerodynamics, AIAA Education Series, 1990.
2.Padfield,G. D., Helicopter Flight Dynamics: The Theory and Application of Flying Qualities and Simulation Modeling, 1995
3. Prouty, R.W., Helicopter Performance, Stability, and Control, Krieger Publishing Company, 1995.
4.Cooke,A.K.,Fitzpatrick, E.W.H., Helicopter Test and Evaluation, AIAA Education Series, 2002.
5.Leishman, J.G., Principles of Helicopter Aerodynamics, Cambridge University Press, 2000.
6. Sevinc C., Development of Forward Flight Trim and Longitudinal Dynamic Stability Codes, Master Thesis, Middle East Technical University, 2009.
7. U.S. Army Helicopter Design Datcom, Volume I – Airfoils, Boeing Doc. No. D210-11097-1, 1976.
8. Hoerner, Fluid Dynamic Drag, Published by Author, 1965.
9. MATLAB Getting Started Guide.
10. MATLAB help files helicopter.

NOMENCLATURE

Symbol Definitions

A	Area , m^2
A 1	1st harmonic lateral cyclic angle
AR	Aspect ratio (-)
B	Tip loss factor
B 1	1^{st} harmonic longitudinal cyclic Angle, deg
D	Fuselage drag, N
D.L.	Disc loading, N
H	H-force, N
HP	Power, hp
I	Inertia, m^4
L	Lift , N
M	Mach number / Pitch moment, N.m
Q	Torque, N.m
R	Radius, m
T	Thrust, N
U	Local velocity component, m/s
V	Forward velocity, m/s
X	Force on X-direction, N
Y	Force on Y-direction, N
Z	Force on Z-direction, N

A	Lift curve slope / Speed of sound, m/s
a 0	Coning angle, deg
a1	Longitudinal flapping w.r.t. the plane of no-feathering
as1	1^{st} harmonic longitudinal flapping angle, deg
b1	Lateral flapping w.r.t. the plane of no-feathering
bs1	1^{st} harmonic lateral flapping angle
c	Chord, m
e	Efficiency factor
f	Flat plate drag area, m^2
g	Gravitational acceleration, m/s^2
h	Height w.r.t. cg, m
I	Incidence, deg
L	Moment arm, m
m	Mass, kg
Q	Dynamic pressure / Pitch rate, Pa, rad/s
υ1	Induced velocity, m/s
υL	Local induced velocity, m/s
x	Displacement in X-direction, m
z	Displacement in Z-direction, m

GREEK LETTER

α Local angle of attack
α_S Shaft angle of attack
α_{TPP} Tip path plane angle of attack
β Angle of sideslip
δ_3 Delta-three angle
ε Downwash angle
γ Lock number / Climb angle
σ Solidity
θ_0 Collective angle
θ_1 Twist angle
λ Inflow ratio wrt the shaft plane
λ' Inflow ratio wrt TPP
μ Advance ratio
ρ Air density
θ Pitch angle
θ_O Collective angle
θ_1 Twist angle
ψ Azimuth angle
υ Local induced velocity
Θ Pitch angle of fuselage
Ω Revolution speed

APPENDIX A

The parameters with bars overhead are the output parameters supplied by a trim analysis

MAIN ROTOR STABILITY DERIVATIVES

$$\frac{\partial \mu}{\partial \dot{x}} = \frac{1}{\Omega R}$$

$$\frac{\partial \lambda'}{\partial \dot{x}} = \frac{1}{\Omega R}\left[\bar{\alpha}_{TPP} - \frac{\sigma}{2\mu}\left(\frac{\partial C_T/\sigma}{\partial \mu} - \frac{C_T/\sigma}{\mu}\right)\right]$$

$$\frac{\partial \lambda'}{\partial \dot{z}} = \frac{1}{\Omega R\left(1 + \frac{\partial C_T/\sigma}{\partial \lambda'}\frac{\sigma}{2\mu}\right)}$$

$$\frac{\partial C_H/\sigma}{\partial a_{1S}} = \frac{\bar{C}_T}{\sigma} + \frac{a}{8}\lambda'$$

$$\frac{\partial a_{1S}}{\partial q} = -\frac{16}{\gamma\Omega\left(1 - e/R\right)^2\left(1 - \mu^2/2\right)} - \frac{12\, e/R}{\gamma\Omega\left(1 - e/R\right)^3\left(1 - \mu^4/4\right)}$$

$$\frac{\partial a_{1S}}{\partial B_1} = -\frac{\left(1 + \frac{3\mu^2}{2}\right)}{\left(1 - \frac{\mu^2}{2}\right)}$$

$$\frac{\partial M}{\partial a_{1S}} = \frac{3}{4}\frac{e}{R}A_b\rho(\Omega R)^2\frac{a}{\gamma}$$

$$\left(\frac{\partial X}{\partial \dot{x}}\right)_M = -A_b\rho(\Omega R)^2\left\{\begin{array}{l}\left[\frac{\partial C_H/\sigma}{\partial \mu} + \frac{\partial C_H/\sigma}{\partial a_{1S}}\frac{\partial a_{1S}}{\partial \mu} + (\bar{a}_{1S} + i_M)\frac{\partial C_T/\sigma}{\partial \mu}\right]\frac{\partial \mu}{\partial \dot{x}} \\ + \left[\frac{\partial C_H/\sigma}{\partial \lambda'} + \frac{\partial C_H/\sigma}{\partial a_{1S}}\frac{\partial a_{1S}}{\partial \lambda'} + (\bar{a}_{1S} + i_M)\frac{\partial C_T/\sigma}{\partial \lambda'}\right]\frac{\partial \lambda'}{\partial \dot{x}}\end{array}\right\}$$

$$\left(\frac{\partial X}{\partial \dot{z}}\right)_M = -A_b\rho(\Omega R)^2\left[\frac{\partial C_H/\sigma}{\partial \lambda'} + \frac{\overline{C}_T}{\sigma}\frac{\partial a_{1S}}{\partial \lambda'} + (\overline{a}_{1S} + i_M)\frac{\partial C_T/\sigma}{\partial \lambda'}\right]\frac{\partial \lambda'}{\partial \dot{z}}$$

$$\left(\frac{\partial X}{\partial q}\right)_M = -A_b\rho(\Omega R)^2\frac{\partial C_H/\sigma}{\partial a_{1S}}\frac{\partial a_{1S}}{\partial q} - \left(\frac{\partial X}{\partial \dot{x}}\right)_M h_M$$

$$\left(\frac{\partial X}{\partial \theta_o}\right)_M = -A_b\rho(\Omega R)^2\left[\frac{\partial C_H/\sigma}{\partial \theta_o} + \frac{\partial C_H/\sigma}{\partial a_{1S}}\frac{\partial a_{1S}}{\partial \theta_o} + (\overline{a}_{1S} + i_M)\frac{\partial C_T/\sigma}{\partial \theta_o}\right]$$

$$\left(\frac{\partial X}{\partial B_1}\right)_M = -A_b\rho(\Omega R)^2\frac{\partial C_H/\sigma}{\partial a_{1S}}\frac{\partial a_{1S}}{\partial B_1}$$

$$\left(\frac{\partial Z}{\partial \dot{x}}\right)_M = -A_b\rho(\Omega R)^2\left[\frac{\partial C_T/\sigma}{\partial \mu}\frac{\partial \mu}{\partial \dot{x}} + \frac{\partial C_T/\sigma}{\partial \lambda'}\frac{\partial \lambda'}{\partial \dot{x}}\right]$$

$$\left(\frac{\partial Z}{\partial \dot{z}}\right)_M = -A_b\rho(\Omega R)^2\frac{\partial C_T/\sigma}{\partial \lambda'}\frac{\partial \lambda'}{\partial \dot{z}}$$

$$\left(\frac{\partial Z}{\partial \theta_o}\right)_M = -A_b\rho(\Omega R)^2\frac{\partial C_T/\sigma}{\partial \theta_o}$$

$$\left(\frac{\partial Z}{\partial B_1}\right)_M = -A_b\rho(\Omega R)^2\frac{\partial C_T/\sigma}{\partial \lambda'}\frac{\partial \lambda'}{\partial a_{1S}}\frac{\partial a_{1S}}{\partial B_1}$$

$$\left(\frac{\partial M}{\partial \dot{x}}\right)_M = \left(\frac{dM}{da_{1S}}\right)_M\left[\frac{\partial a_{1S}}{\partial \mu}\frac{\partial \mu}{\partial \dot{x}} + \frac{\partial a_{1S}}{\partial \lambda'}\frac{\partial \lambda'}{\partial \dot{x}}\right] - \left(\frac{\partial X}{\partial \dot{x}}\right)_M h_M + \left(\frac{\partial Z}{\partial \dot{x}}\right)_M l_M$$

$$\left(\frac{\partial M}{\partial \dot{z}}\right)_M = \left(\frac{dM}{da_{1S}}\right)_M\frac{\partial a_{1S}}{\partial \lambda'}\frac{\partial \lambda'}{\partial \dot{z}} - \left(\frac{\partial X}{\partial \dot{z}}\right)_M h_M + \left(\frac{\partial Z}{\partial \dot{z}}\right)_M l_M$$

$$\left(\frac{\partial M}{\partial q}\right)_M = \left(\frac{dM}{da_{1S}}\right)_M\frac{\partial a_{1S}}{\partial q} - \left(\frac{\partial X}{\partial q}\right)_M h_M$$

$$\left(\frac{\partial M}{\partial \theta_o}\right)_M = \left(\frac{dM}{da_{1S}}\right)_M\frac{\partial a_{1S}}{\partial \theta_o} - \left(\frac{\partial X}{\partial \theta_o}\right)_M h_M + \left(\frac{\partial Z}{\partial \theta_o}\right)_M l_M$$

$$\left(\frac{\partial M}{\partial B_1}\right)_M = \left(\frac{dM}{da_{1S}}\right)_M\frac{\partial a_{1S}}{\partial B_1} - \left(\frac{\partial X}{\partial B_1}\right)_M h_M$$

HORIZONTAL STABILIZER STABILITY DERIVATIVES

$$\frac{\partial \gamma_c}{\partial \dot{z}} = -\frac{1}{V}$$

$$\frac{\partial \varepsilon_{M_H}}{\partial \dot{x}} = \frac{\upsilon_H}{\upsilon_1}\frac{1}{4qA_M}\left[-\left(\frac{\partial Z}{\partial \dot{x}}\right)_M + \frac{2\overline{Z}_M}{V}\right]$$

$$\frac{\partial \varepsilon_{M_H}}{\partial \dot{z}} = -\frac{\upsilon_H}{\upsilon_1}\frac{1}{4qA_M}\left(\frac{\partial Z}{\partial \dot{z}}\right)_M$$

$$\frac{\partial \varepsilon_{F_H}}{\partial \dot{z}} = \frac{d\varepsilon_{F_H}}{d\alpha_F}\left[\frac{1}{4qA_M}\left(\frac{\partial Z}{\partial \dot{z}}\right)_M - \frac{\partial \gamma_c}{\partial \dot{z}}\right]$$

$$\frac{\partial \alpha_H}{\partial \dot{x}} = -\frac{\partial \varepsilon_{M_H}}{\partial \dot{x}}$$

$$\frac{\partial \alpha_H}{\partial \dot{z}} = -\left[\frac{\partial \varepsilon_{M_H}}{\partial \dot{z}} + \frac{\partial \varepsilon_{F_H}}{\partial \dot{z}} + \frac{\partial \gamma_c}{\partial \dot{z}}\right]$$

$$\frac{\partial \alpha_H}{\partial \ddot{z}} = -\left[\frac{\partial \varepsilon_{M_H}}{\partial \dot{z}}\right]\frac{l_H}{V}$$

$$\left(\frac{\partial X}{\partial \dot{x}}\right)_H = \left\{\frac{2}{V}X_H + \frac{q_H}{q}qA_H a_H \begin{Bmatrix}\left(\overline{\alpha}_H - \alpha_{L=0_H}\right)\left[1 - \dfrac{2a_H\left(1+\delta_{i_H}\right)}{\pi A.R._H}\right] \\ +\left(\overline{\alpha}_H - i_H\right)\end{Bmatrix}\right\}\frac{\partial \alpha_H}{\partial \dot{x}}$$

$$\left(\frac{\partial X}{\partial \dot{z}}\right)_H = \frac{q_H}{q}qA_H a_H\left\{\left(\overline{\alpha}_H - \alpha_{L=0_H}\right)\left[1 - \frac{2a_H\left(1+\delta_{i_H}\right)}{\pi A.R._H}\right] + \left(\overline{\alpha}_H - i_H\right)\right\}\frac{\partial \alpha_H}{\partial \dot{z}}$$

$$\left(\frac{\partial X}{\partial \ddot{z}}\right)_H = \left(\frac{\partial X}{\partial \dot{z}}\right)_H \frac{\dfrac{\partial \alpha_H}{\partial \ddot{z}}}{\dfrac{\partial \alpha_H}{\partial \dot{z}}}$$

$$\left(\frac{\partial Z}{\partial \dot{x}}\right)_H = \left\{\begin{matrix}\dfrac{2}{V}\overline{Z}_H \\ +\dfrac{q_H}{q}qA_H a_H \begin{Bmatrix}1 + \dfrac{a_H\left(1+\delta_{i_H}\right)}{\pi A.R._H}\begin{bmatrix}2\left(\overline{\alpha}_H - \alpha_{L=0_H}\right)\left(\overline{\alpha}_H - i_H\right) \\ +\left(\overline{\alpha}_H - \alpha_{L=0_H}\right)^2\end{bmatrix} \\ +c_{D_{o,H}}\end{Bmatrix}\end{matrix}\right\}\frac{\partial \alpha_H}{\partial \dot{x}}$$

$$\left(\frac{\partial Z}{\partial \dot{z}}\right)_H = -\frac{q_H}{q}qA_H a_H\left\{1 + \frac{a_H\left(1+\delta_{i_H}\right)}{\pi A.R._H}\begin{bmatrix}2\left(\overline{\alpha}_H - \alpha_{L=0_H}\right)\left(\overline{\alpha}_H - i_H\right) \\ +\left(\overline{\alpha}_H - \alpha_{L=0_H}\right)^2\end{bmatrix} + c_{D_{o,H}}\right\}\frac{\partial \alpha_H}{\partial \dot{z}}$$

$$\left(\frac{\partial Z}{\partial \ddot{z}}\right)_H = \left(\frac{\partial Z}{\partial \dot{z}}\right)_H \frac{\frac{\partial \alpha_H}{\partial \ddot{z}}}{\frac{\partial \alpha_H}{\partial \dot{z}}}$$

$$\left(\frac{\partial Z}{\partial q}\right)_H = \left(\frac{\partial Z}{\partial \dot{z}}\right)_H l_H$$

$$\left(\frac{\partial M}{\partial \dot{x}}\right)_H = -\left(\frac{\partial X}{\partial \dot{x}}\right)_H h_H + \left(\frac{\partial Z}{\partial \dot{x}}\right)_H l_H$$

$$\left(\frac{\partial M}{\partial \dot{z}}\right)_H = -\left(\frac{\partial X}{\partial \dot{z}}\right)_H h_H + \left(\frac{\partial Z}{\partial \dot{z}}\right)_H l_H$$

$$\left(\frac{\partial M}{\partial \ddot{z}}\right)_H = -\left(\frac{\partial X}{\partial \ddot{z}}\right)_H h_H + \left(\frac{\partial Z}{\partial \ddot{z}}\right)_H l_H$$

$$\left(\frac{\partial M}{\partial q}\right)_H = \left(\frac{\partial Z}{\partial q}\right)_H l_H$$

VERTICAL STABILIZER STABILITY DERIVATIVES

$$\left(\frac{\partial X}{\partial \dot{x}}\right)_V = \frac{2}{V}\left[\overline{X}_V + 2\Delta\overline{D}_{V_{\text{int}}}\right]$$

Where $_{V\text{int}}\ \Delta D$ is the additional drag coming from the interference effect between the vertical stabilizer and the tail rotor:

$$\Delta\overline{D}_{V_{\text{int}}} = \frac{8}{\pi q}\left|\frac{T_T}{2R_T}\frac{Y_V}{b_V}\right|K_{\text{int}}$$

FUSELAGE STABILITY DERIVATIVES

$$\frac{\partial \gamma_c}{\partial \dot{z}} = -\frac{1}{V}$$

$$\frac{\partial \varepsilon_{M_F}}{\partial \dot{x}} = \frac{\upsilon_F}{\upsilon_1}\frac{1}{4qA_M}\left[-\left(\frac{\partial Z}{\partial \dot{x}}\right)_M + \frac{2\overline{Z}_M}{V}\right]$$

$$\frac{\partial \varepsilon_{M_F}}{\partial \dot{z}} = -\frac{\upsilon_F}{\upsilon_1}\frac{1}{4qA_M}\left(\frac{\partial Z}{\partial \dot{z}}\right)_M$$

$$\frac{\partial \alpha_F}{\partial \dot{x}} = -\frac{\partial \varepsilon_{M_F}}{\partial \dot{x}}$$

$$\frac{\partial \alpha_F}{\partial \dot{z}} = -\left[\frac{\partial \varepsilon_{M_F}}{\partial \dot{z}} + \frac{\partial \gamma_c}{\partial \dot{z}}\right]$$

$$\left(\frac{\partial X}{\partial \dot{x}}\right)_F = \frac{2}{V}\overline{X}_F$$

$$\left(\frac{\partial X}{\partial \dot{z}}\right)_F = \left(\overline{L}_F - q\frac{\partial f}{\partial \alpha_F}\right)\frac{\partial \alpha_F}{\partial \dot{z}}$$

$$\left(\frac{\partial Z}{\partial \dot{x}}\right)_F = \frac{2}{V}\overline{Z}_F$$

$$\left(\frac{\partial Z}{\partial \dot{z}}\right)_F = -\left(\overline{D}_F + q\frac{\partial L/q}{\partial \alpha_F}\right)\frac{\partial \alpha_F}{\partial \dot{z}}$$

$$\left(\frac{\partial M}{\partial \dot{x}}\right)_F = \frac{2}{V}\overline{M}_F + q\frac{\partial M/q}{\partial \alpha_F}\frac{\partial \alpha_F}{\partial \dot{x}}$$

$$\left(\frac{\partial M}{\partial \dot{z}}\right)_F = q\frac{\partial M/q}{\partial \alpha_F}\frac{\partial \alpha_F}{\partial \dot{z}}$$

TOTAL STABILITY DERIVATIVES

The total derivatives are found by adding the corresponding terms of main rotor, tail rotor, empennage and the fuselage:

$$\frac{\partial X_i}{\partial x_i} = \left(\frac{\partial X_i}{\partial x_i}\right)_M + \left(\frac{\partial X_i}{\partial x_i}\right)_T + \left(\frac{\partial X_i}{\partial x_i}\right)_{HS} + \left(\frac{\partial X_i}{\partial x_i}\right)_{VS} + \left(\frac{\partial X_i}{\partial x_i}\right)_F$$

Where $Xi = X\ Z\ M$

TRIM EQUATIONS

Harmonic pitch angles are found using the first harmonic flapping angles

$$A_1 = b_{1s} - \frac{\left[a_0\left(\frac{4}{3}\mu + \frac{16}{45\pi}\mu^4\right) + \frac{\upsilon_1}{\Omega R}\left(1 + \frac{\mu^4}{24}\right)\right]}{\left(1 + \frac{\mu^2}{2} - \frac{\mu^4}{24}\right)}$$

$$B_1 = -a_{1s} + \frac{\mu\left[\left(\frac{8}{3} + \frac{32}{45}\frac{\mu^3}{\pi}\right)\theta_0 + \left(2 + \frac{\mu^4}{12}\right)\theta_1 + \left(2 - \frac{\mu^2}{2}\right)\lambda'\right]}{\left(1 + \frac{3}{2}\mu^2 - \frac{5\mu^4}{24}\right)}$$

The total thrust force is calculated by multiplying the lift by the number of blades.

$$T_M = \frac{bR}{2\pi}\left\{\int_0^{\pi}\int_{x_0}^{B}\frac{\Delta L}{\Delta r}d\frac{r}{R}.d\psi + \int_{\pi-\mu\sin\psi}^{2\pi}\int^{B}\frac{\Delta L}{\Delta r}d\frac{r}{R}.d\psi - \int_{\pi}^{2\pi-\mu\sin\psi}\int_{x_0}\frac{\Delta L}{\Delta r}d\frac{r}{R}.d\psi\right\}$$

Where L lift force on each bald and B is the loses factor station, this is for eliminate the root and tip losses. The reverse flow region defined by μsinψ.

The local angle of attack is defined as ;

$$\alpha = \theta + \tan^{-1}\left(\frac{U_P}{U_T}\right)$$

Introducing the pitch angle

$$\theta = \theta_0 + \frac{r}{R}\theta_1 - A_1\cos\psi - B_1\sin\psi$$

The tangential velocity component is

$$\overline{U}_T = \frac{r}{R} + \mu \sin\psi$$

The vertical velocity component is

$$U_P = V\alpha_S - \upsilon_L - r\dot{\beta} - V\beta\cos\psi$$

The flapping angle is

$$\beta = a_0 - a_{1S}\cos\psi - b_{1S}\sin\psi$$
$$\dot{\beta} = \left(a_{1S}\sin\psi - b_{1S}\cos\psi\right)\Omega$$

So that the collective angle becomes

$$\theta_0 = \frac{\left(\begin{array}{l}\left(\frac{4}{a}\left(1+\frac{3}{2}\mu^2-\frac{5}{24}\mu^4\right)C_T/\sigma - \left(1-\frac{3}{2}\mu^2+\frac{\mu^4}{6}-\frac{9}{16}\mu^6-\frac{3}{192}\mu^8\right)\frac{\theta_1}{2}\right) \\ -\left(1+\frac{13}{24}\mu^4+\frac{\mu^6}{48}\right)\lambda'\end{array}\right)}{\left(\frac{2}{3}-\frac{2}{3}\mu^2-\frac{8}{9\pi}\mu^3+\frac{25}{36}\mu^4-\frac{92}{45\pi}\mu^5-\frac{5}{24}\mu^6+\frac{\mu^7}{135\pi}\right)}$$

TOTAL FORCES AND MOMENTS

The forces and moments can be calculated by the following formulas;

$$X_M = -\overline{H}_{a_{1S}=0_M} - \overline{T}_M a_{1S} - T_M i_M$$
$$X_T = -\overline{H}_T$$
$$X_H = \overline{L}_H\left(\alpha_H - \varepsilon_{F_H}\right) - \overline{L}_H a_H\left(\begin{array}{l}\alpha_H + i_H \\ -\alpha_{L=0_H} - \varepsilon_{F_H}\end{array}\right)\frac{\left(1+\delta_{i_H}\right)}{\pi A R_H} - q\frac{q_H}{q}A_H C_{D_{0,H}}$$
$$X_V = -\overline{D}_V - \overline{L}_V\left(\eta_{M_V} + \eta_{T_V}\right)$$
$$X_F = -\overline{D}_F + \overline{L}_F\alpha_F$$

$$Z_M = -T_M$$
$$Z_T = \overline{b}_{1S_T}\overline{T}_T$$
$$Z_H = -q\frac{q_H}{q}A_H a_H\left(\alpha_H + i_H - \alpha_{L=0_H} - \varepsilon_{F_H}\right) - \overline{D}_H\left(\alpha_H - \varepsilon_{F_H}\right)$$
$$Z_V = -\left(\overline{D}_V + \overline{L}_V\left(\eta_{M_V} + \eta_{F_V}\right)\right)\left(\Theta - \frac{\upsilon_V}{\upsilon_1}\frac{T_M}{4qA_M} - \varepsilon_{F_V}\right)$$

$$Z_F = -q\left(\left(L_F/q\right)_{\alpha_F=0} + \frac{\partial\left(L_F/q\right)}{\partial\alpha_F}\alpha_F\right) - \overline{D}_F\alpha_F$$

$$M_M = \frac{\partial M}{\partial a_{1S}}a_{1S}$$

$$M_T = -\overline{Q}_T$$

$$M_F = q\left(\left(M_F/q\right)_{\alpha_F=0} + \frac{\partial\left(M_F/q\right)}{\partial\alpha_F}\alpha_F\right)$$

The total force and moments are;

$$\sum X = X_M + X_T + X_H + X_V + X_F - W\Theta = 0$$

$$\sum Z = Z_M + Z_T + Z_H + Z_V + Z_F + W = 0$$

$$\sum M = \begin{pmatrix} M_M + M_T + M_F - X_M h_M + Z_M l_M - X_T h_T \\ + Z_T l_T - X_H h_H + Z_H l_H - X_V h_V + Z_F l_F - X_F h_F \end{pmatrix} = 0$$